In Proceedings of the Fifth International High-Level Radioactive Waste Management Conference," May 22-26, Las Vegas, USA.

FRACTURE-MATRIX INTERACTION IN TOPOPAH SPRING TUFF: EXPERIMENT AND NUMERICAL ANALYSIS

Robert J. Glass and Vince C. Tidwell
Geohydrology Division 6115
Sandia National Laboratories
Albuquerque, NM 87185

Alan L. Flint
United States Geological Survey
Yucca Mountain Project
Nevada Test Site, NV 89023

William Peplinski
Spectra Research Institute
1613 University Blvd. NE
Albuquerque, NM 87102

Yvette Castro
University of Purabo
Department of Engineering
Caguas, PR 00726-5734

ABSTRACT

Fracture-matrix interaction is investigated through combined physical and numerical experimentation. Two slabs of Topopah Spring Tuff are mated to form a vertical saw cut fracture to which water is supplied. X-ray imaging is used to obtain the matrix porosity field and transient saturation fields as water moves from the fracture into the matrix. Porosity, hydraulic conductivity, and pressure/saturation relations of the matrix are measured on small cores taken from adjacent rock. Correlations between hydraulic properties and porosity are developed and modeled. Numerical simulations using TOUGH2[1] are accomplished with a series of property fields of increasing detail. Property fields are modeled using the measured porosity field divided into 1, 3, 5, 11, and 21 porosity groups with the hydraulic properties assigned from the developed correlations and the average porosity within each group. Comparison with experimental results allows us to begin to evaluate current matrix property measurement techniques, specific matrix property models, property estimation procedures, and effects of matrix property variability.

INTRODUCTION

Estimates of ground water travel time through unsaturated fractured rock such as that at Yucca Mountain, Nevada are expected to be very sensitive to the nature and degree of fracture-matrix interaction. In efforts to predict ground water travel times, Total Systems Performance Assessment exercises are currently using two models that incorporate fracture-matrix interaction in very different ways[2]. The first conceptual model assumes equilibrium between the fractures and the matrix and uses capillary bundle theory to build an effective media[3]. The second model assumes fractures not to interact with the matrix thus forming conduits for all flow from the surface. In both of these abstractions, many features of flow in fractures and fracture matrix interaction are neglected[4,5,6,7,8]. As such, questions concerning the suitability of current treatments of fracture-matrix interaction have been raised that can only be addressed with the support of physical observations in the field and laboratory.

It is in this spirit that Foltz et al.[9] presented the results of a preliminary investigation of fracture-matrix interaction using Timber Mountain Tuff and controlled property, fabricated rocks (sintered glass bead packs). They demonstrated the use of x-ray absorption techniques to acquire two-dimensional saturation fields formed by matrix imbibition of fluid from a saw cut fracture. Linear behavior with the square root of time of the saturation profile translation and the total imbibition into the rock matrix from the fracture demonstrated applicability of the nonlinear diffusion equation (general form of Richard's equation) to describe water imbibition into unsaturated tuff. Further comparisons of theory and experiment were precluded because hydraulic properties of the tuff slab were not measured.

In the study presented here, we build on the former work of Foltz et al. by conducting a similar fracture-matrix experiment in a slab of Topopah Spring tuff. In contrast to the former experiment, porosity, hydraulic conductivity, and pressure/saturation relations are measured on small cores taken from adjacent rock. Correlations between hydraulic properties and porosity are found and modeled. Numerical simulations using TOUGH2[1] are accomplished with a series of property fields of increasing detail. Property fields were modeled using the measured porosity field divided into 1, 3, 5, 11, and 21 porosity groups with the hydraulic properties assigned from the developed correlations and the average porosity within each group. Comparison between numerical simulation and experimental results allows us a means to evaluate current matrix property measurement techniques, specific matrix property models, property estimation procedures, and effects of matrix property variability on fracture-matrix interaction.

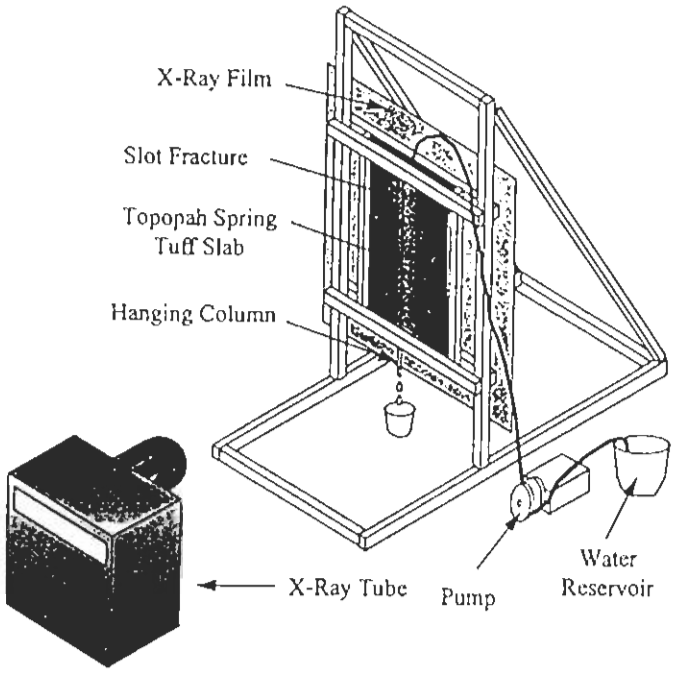

Figure 1: Schematic of fracture-matrix experimental setup.

FRACTURE-MATRIX EXPERIMENT

Two pieces of rock (each measuring roughly 50 cm high, 15 cm wide and 2.5 cm thick) were cut from a single slab of Topopah Spring Tuff (from Busted Butte on the Nevada Test Site). The two pieces were mated to create a single 0.1 mm slot fracture forming a simple two-dimensional thin slab system oriented normal to the plane of the fracture (Figures 1 and 2). A key characteristic of the tuff slabs (visible in Figure 2) is the horizontal, flattened pumice inclusions oriented normal to the fracture. The test system was wrapped in mylar to minimize evaporation during the course of the experiment. A constant flux boundary condition was applied at the top of the fracture (2.6 ml/min) through two needles inserted into the fracture and a constant suction boundary (7 cm water) was applied at the bottom of the fracture with a hanging water column.

At the onset of infiltration, water moved rapidly through the fracture and began to drip from the bottom of the hanging column tube. Water in the fracture did not fully span the fracture and instead fingered within the 2.5 cm fracture depth. The experiment progressed until the wetting fronts had fully spanned the width of the matrix blocks. During this period, two dimensional saturation fields integrated over the thickness of the slab were imaged at 5, 15, 30, 60, 120 and 180 minutes by means of an x-ray absorption technique[10] (see Figures 1 and 2). Potassium iodide (KI) was dissolved in the water (10% by weight) to enhance the x-ray adsorption contrast between air and water. A constant density wedge was included in each image to allow image adjustment for optical

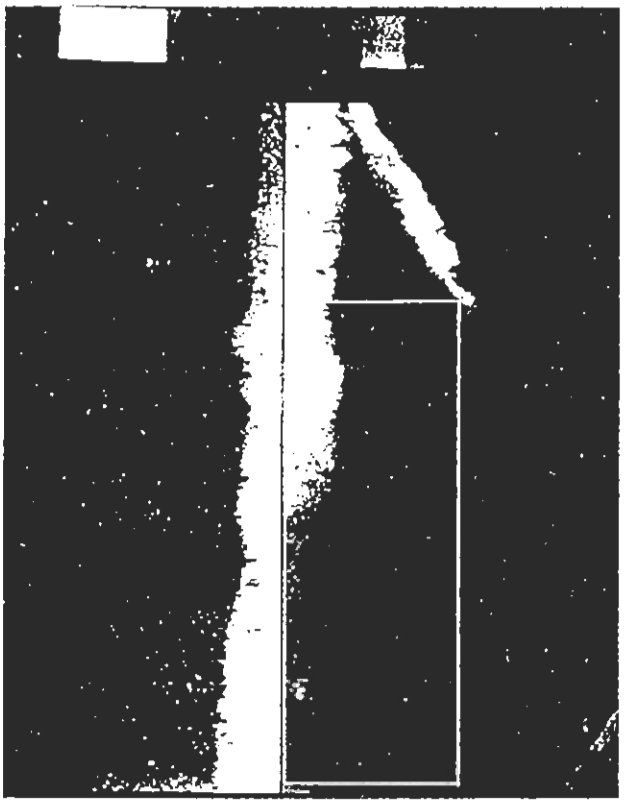

Figure 2: Digitized x-ray image acquired during the fracture-matrix experiment. Light areas along the fracture represent water imbibing into the tuff matrix. Boxed region depicts region analyzed.

density shifts that can occur during film processing and digitization. Following the experiment, the blocks were rinsed for several weeks to remove all KI, then oven dried followed by vacuum saturating with the KI solution, and finally re-imaged to yield the fully saturated field.

X-ray film was digitized using an electronically cooled digital camera into 1317x1035 pixels (0.44 mm x0.44 mm) with a dynamic greyscale range of 4096 levels (Figure 2).
A subsection of the experiment 800 pixels tall and 580 wide (352 mm tall, 255.2 mm wide) was chosen for subsequent analysis. To facilitate analysis, this region was split into two halves with a 4 pixel wide zone (1.76 mm) at the fracture removed to yield two blocks 800 pixels tall and 288 wide (352 mm tall, 126.72 mm wide). The porosity field and saturation fields as a function of time were then calculated for the two blocks from the digitized images using the method of Tidwell and Glass[10]. To facilitate numerical simulation (i.e., minimize the computational burden), data were reduced to a lower spatial resolution of 50 by 18 points (factor of 1/16, 900 points 7.04 mm square) through arithmetic averaging appropriate for the extensive properties of porosity and saturation. For brevity sake, only results for the right hand side block will be presented here. Figure 3 presents the saturation fields at low spatial resolution for 5, 30, 60, and

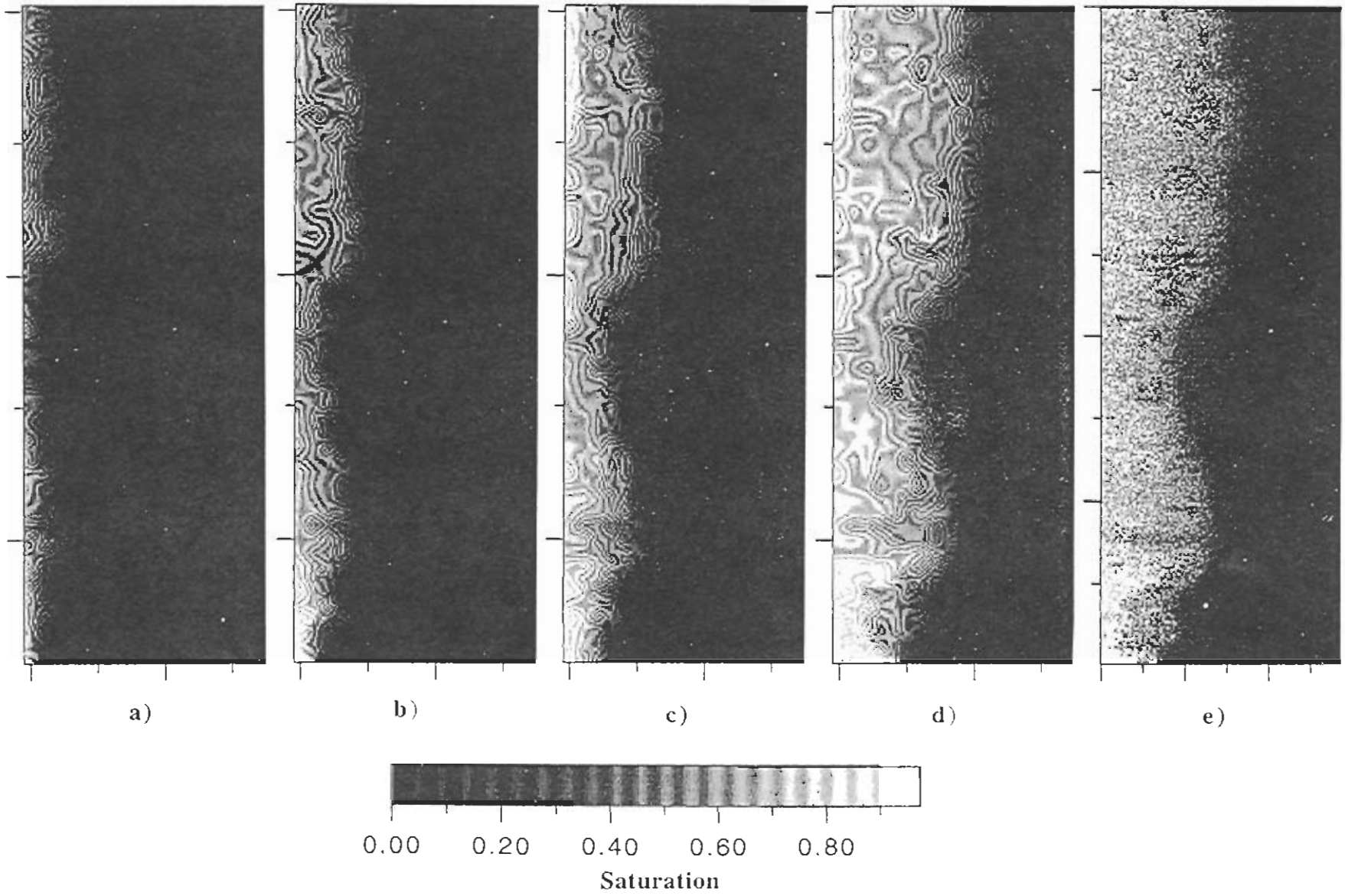

Figure 3: Observed saturation fields for the right hand block at a) 5 minutes, b) 30 minutes, c) 60 minutes and d) 180 minutes at low resolution (50 by 18 grid). The 180 minute image at full resolution (800 by 288 points) is shown for comparison in e).

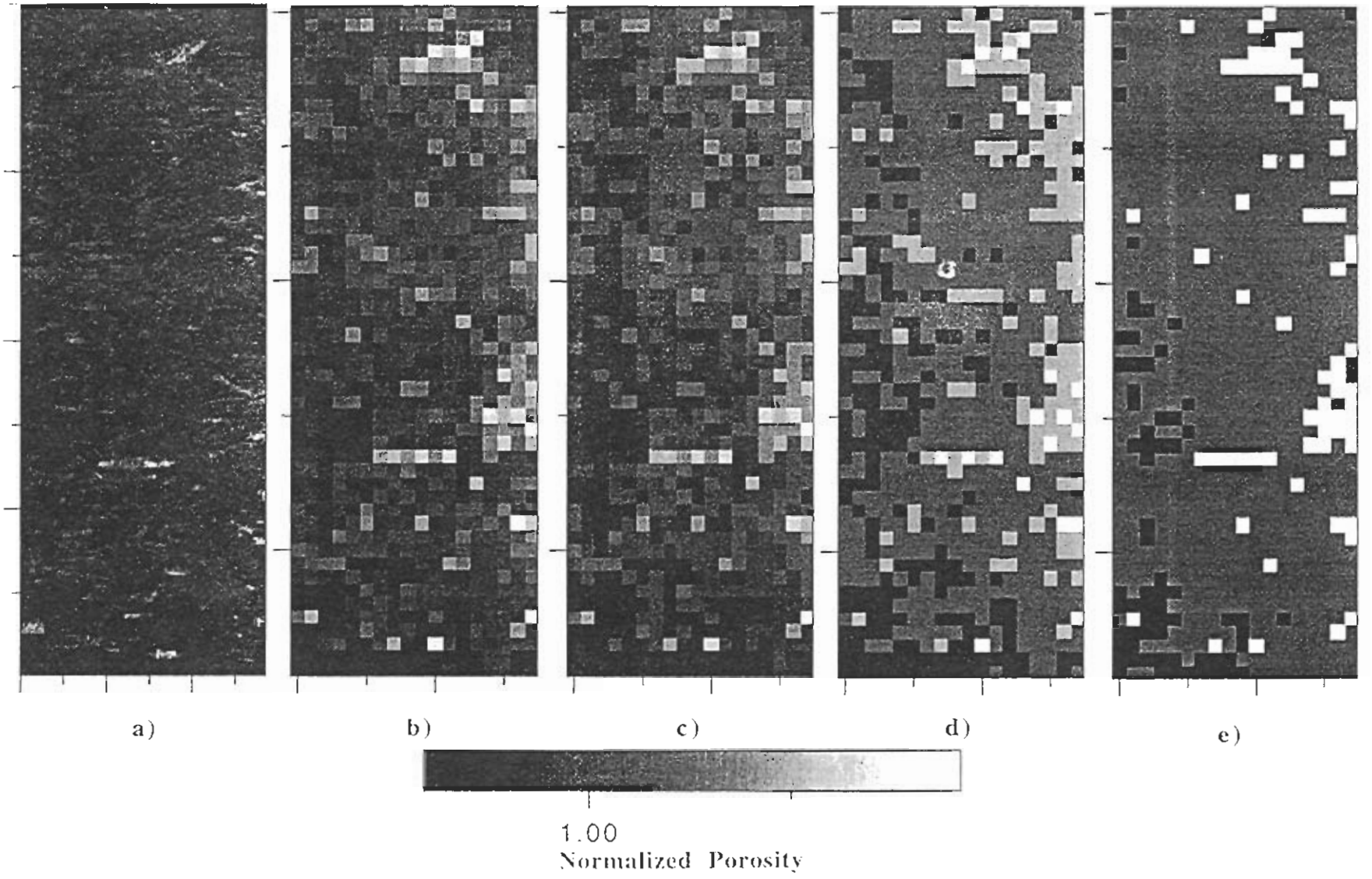

Figure 4: Normalized porosity fields for the right hand block at a) high resolution. Low resolution (50 by 18 grid) normalized porosity fields with b) 21 hydraulic property classes, c) 11 hydraulic property classes, d) 5 hydraulic property classes, and e) 3 hydraulic property classes. Porosity was normalized by the mean porosity value. See Numerical Simulation section for discussion of hydraulic property classes.

180 minutes. For comparison, the full resolution image at 180 minutes is shown in Figure 3c.

The porosity field normalized by the average value for both full and low spatial resolution is shown in Figure 4. Average porosity for the block was determined gravimetrically to be .20 +-.005. The variance of the normalized porosity field was found to be invariant with scale between the full resolution image (0.44 mm) and the 50 by 18 grid resolution (7.04 mm). Variograms were calculated for the two principal axes of the porosity field, parallel and normal to the fracture. In the direction parallel to the fracture a noticeable hole effect is present. This behavior is due to periodicity in the structure of the rock caused by numerous flattened pumice inclusions oriented normal to this principal axis. The correlation length scale is noted to increase from 30 mm at the highest image resolution to about 50 mm at the lowest resolution; however, the hole structure is preserved. Normal to the fracture, a strong exponential behavior without the hole effect is exhibited. A correlation length scale of approximately 30 mm is maintained regardless of image resolution for this principal axis.

HYDRAULIC PROPERTY MEASUREMENT AND MODELING

Ten plugs (2.5 cm diameter) cored from rock samples trimmed from the slab were tested in the laboratory to obtain porosity, saturated hydraulic conductivity (K), and drainage pressure/saturation curves. Porosity measurements were accomplished using gravimetric methods while the saturated hydraulic conductivity was measured using a constant head permeameter. Pressure/saturation curves were measured using air drying and a chilled mirror psychrometer over the range of 0 to -200 MPa. The van Genuchten[11] form of the moisture release curve was subsequently fit to the data and its parameters, alpha and n (with m=1-1/n), were calculated. Relative permeability was not measured directly, and therefore, was modeled using the mapping of Mualem[12] from the saturation/pressure relation.

Characterization of the rock cores yielded porosity values from 0.07 to 0.25 and saturated hydraulic conductivities of 3.6 E-8 to 2.3 E-4 cm/sec. In order to relate hydraulic properties measured on the rock cores to the tuff slabs used in the experiment, correlations between porosity and alpha, n, and K were explored (Figures 5a, b, and c, respectively). Functional forms given in the figures were fit to the data by the least squares method to quantify the desired relations. Once the porosity was known the functional relations were used to predict alpha, n, and K and hence model the van Genuchten forms of the moisture release curves. Comparison of fitted and modeled moisture release curves for the best and worst match are presented in Figure 6.

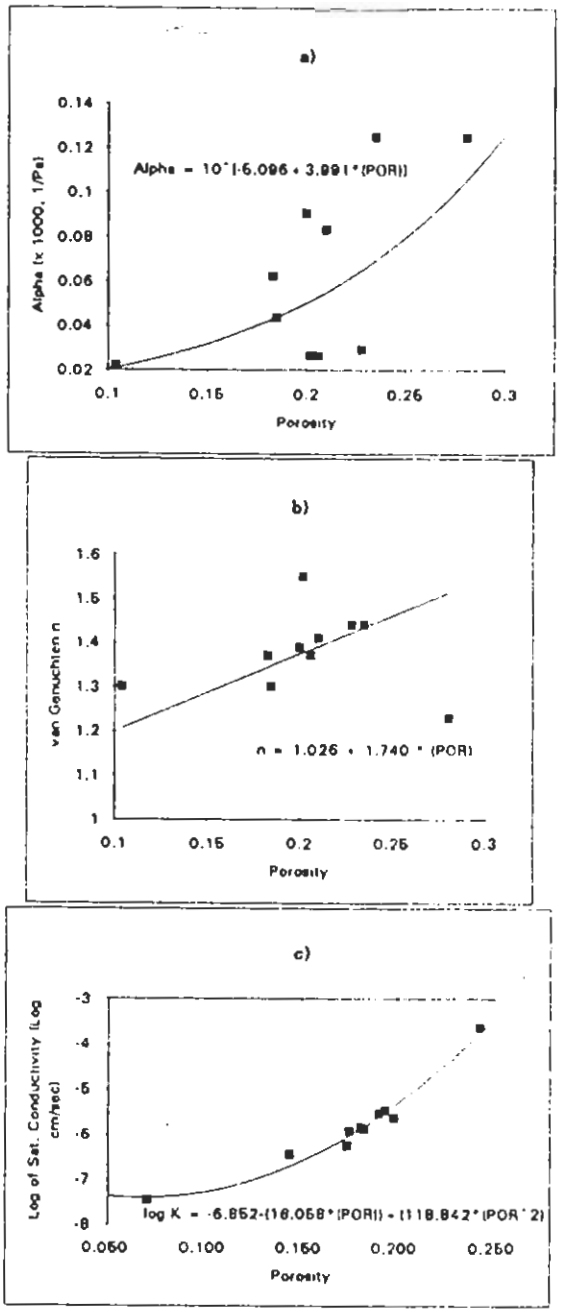

Figure 5: Correlations between porosity and a) alpha, b) n, and c) saturated hydraulic conductivity.

NUMERICAL SIMULATION

Two dimensional deterministic simulations of the right hand side of the experiment were accomplished using TOUGH2 on the low resolution 50 by 18 grid. Five property fields of decreasing detail were investigated. To develop these fields, the porosity histogram was divided into 21, 11, 5, 3 and 1 hydraulic property classes spanning equal porosity increments of 1/21, 1/11, 1/5, 1/3 and 1 of the full porosity range. The value of the porosity at the midpoint of each increment was used for calculating the properties of the increment. Discrete

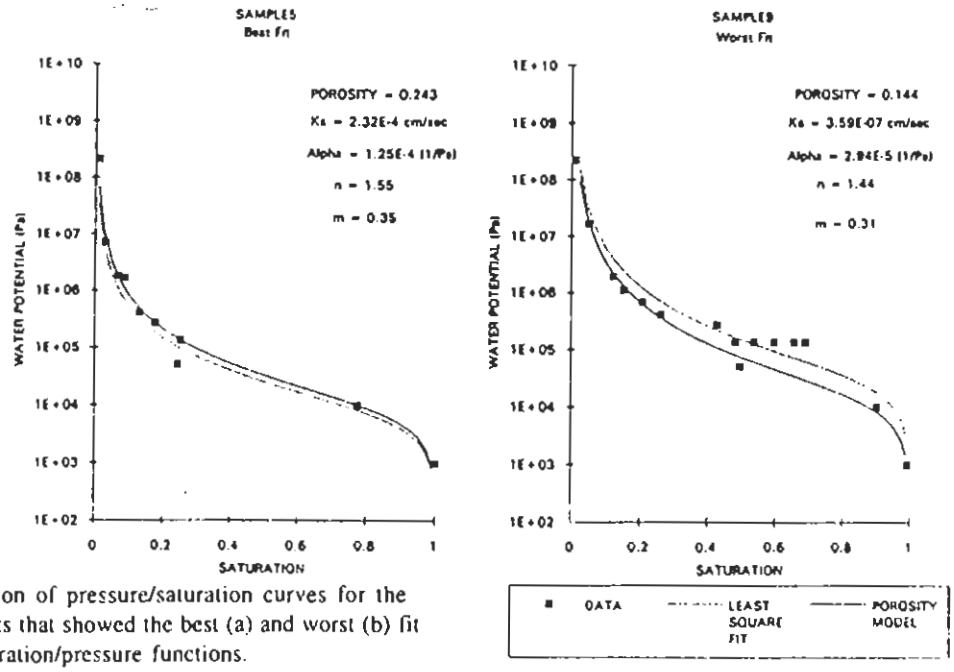

Figure 6: Comparison of pressure/saturation curves for the sample measurements that showed the best (a) and worst (b) fit of the modeled saturation/pressure functions.

porosity fields for the 21, 11, 5 and 3 groups are shown in Figures 4b, c, d and e, respectively. Other hydraulic property fields used for input to TOUGH2 were calculated from these fields by the fitted correlation functions discussed above. Saturation fields (time=180 minutes) simulated for each of the five different property fields are presented in Figure 7.

COMPARISON OF EXPERIMENT AND SIMULATION

Saturation fields simulated numerically are compared with the physical experiment at two levels of detail: the average moisture content integrated over the full region of analysis and the spatial variation of the saturation field within.

The overall average moisture content as a function of time for the modeled subregion of the experiment and the five numerical simulations is presented in Figure 8. From this graph it is apparent that the numerical simulations over predict the average moisture content at early times by a factor of two to three; however, at later times the simulations approach the measured values to within 20%. One source of this discrepancy is the low resolution of the simulation grid (50 by 18). This resolution does not adequately capture the details of the property field nor the steep gradients driving flow within the field (note fine scale detail in Figure 3e). This is especially obvious adjacent to the fracture. Highly porous pumice grains that intersect the fracture effectively increase the fracture surface area, thus enhancing imbibition. In contrast, pumice grains close to the fracture but not intersecting act as capillary barriers which inhibit imbibition.

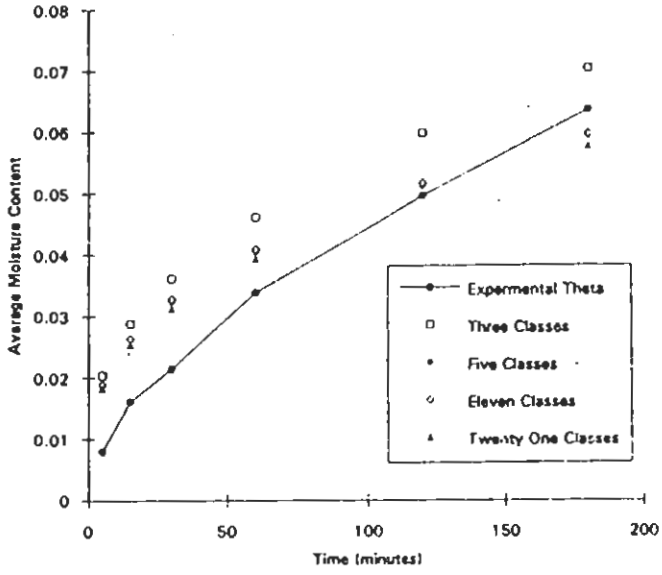

Figure 8: Average moisture content as a function of time for experiment and simulations.

Low resolution (50 by 18) experimental and simulated saturation fields are subtracted and the differences are plotted in banded greyscale in Figure 9. Light regions between bands indicate where the simulation under predicts the experimental data, while dark regions indicate where the simulation over predicts observed system response. In all cases, simulations over predict saturation behind the wetting front and near the fracture. This occurs in part because the functional forms used for the pressure/saturation and relative permeability do not

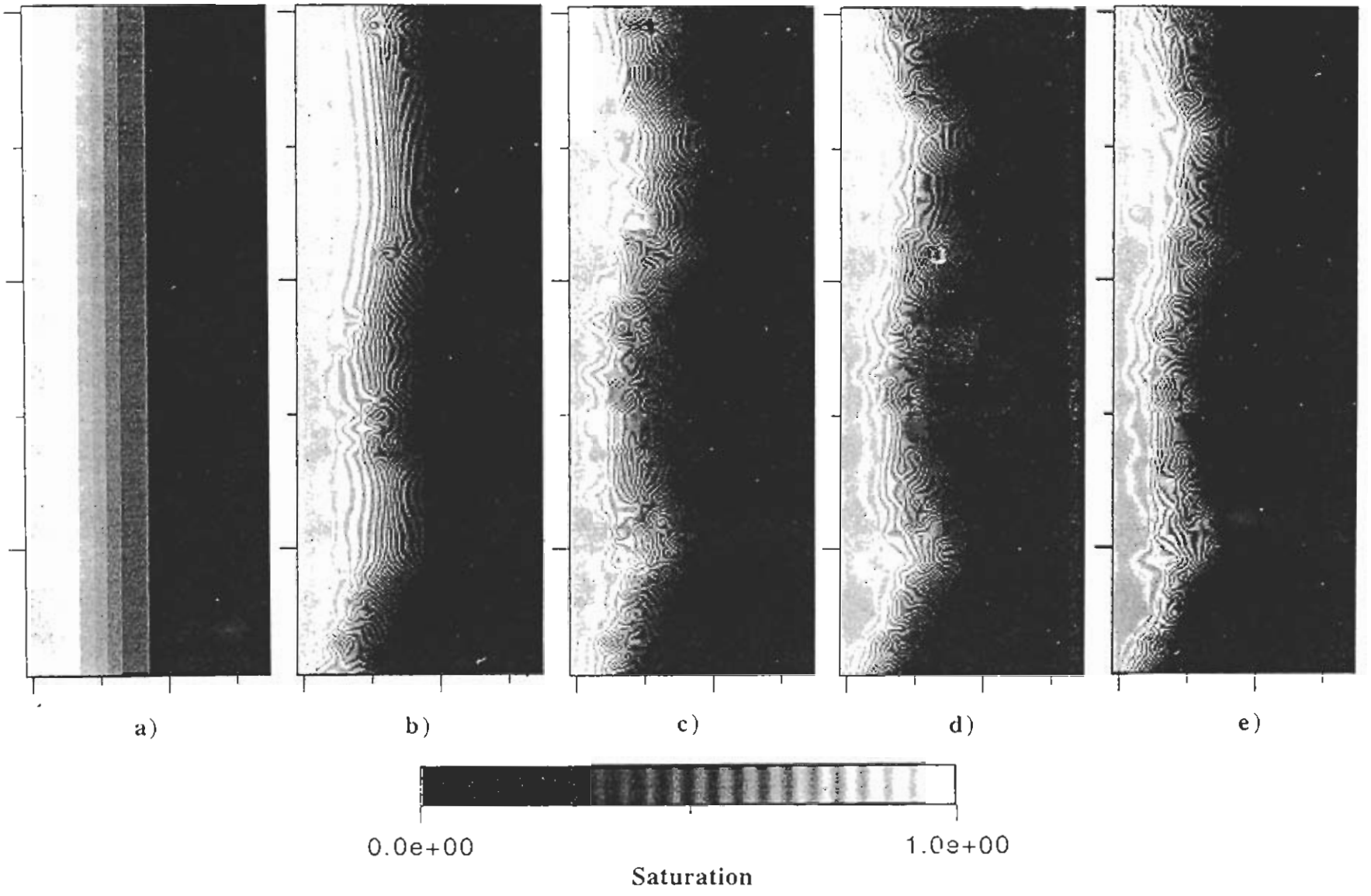

Figure 7: Simulated saturation fields for a) 1, b) 3, c) 5, d) 11, and e) 21 hydraulic property classes (time=180 minutes). Note that the pattern of saturation does not increase in complexity appreciably with hydraulic property classes greater than 5.

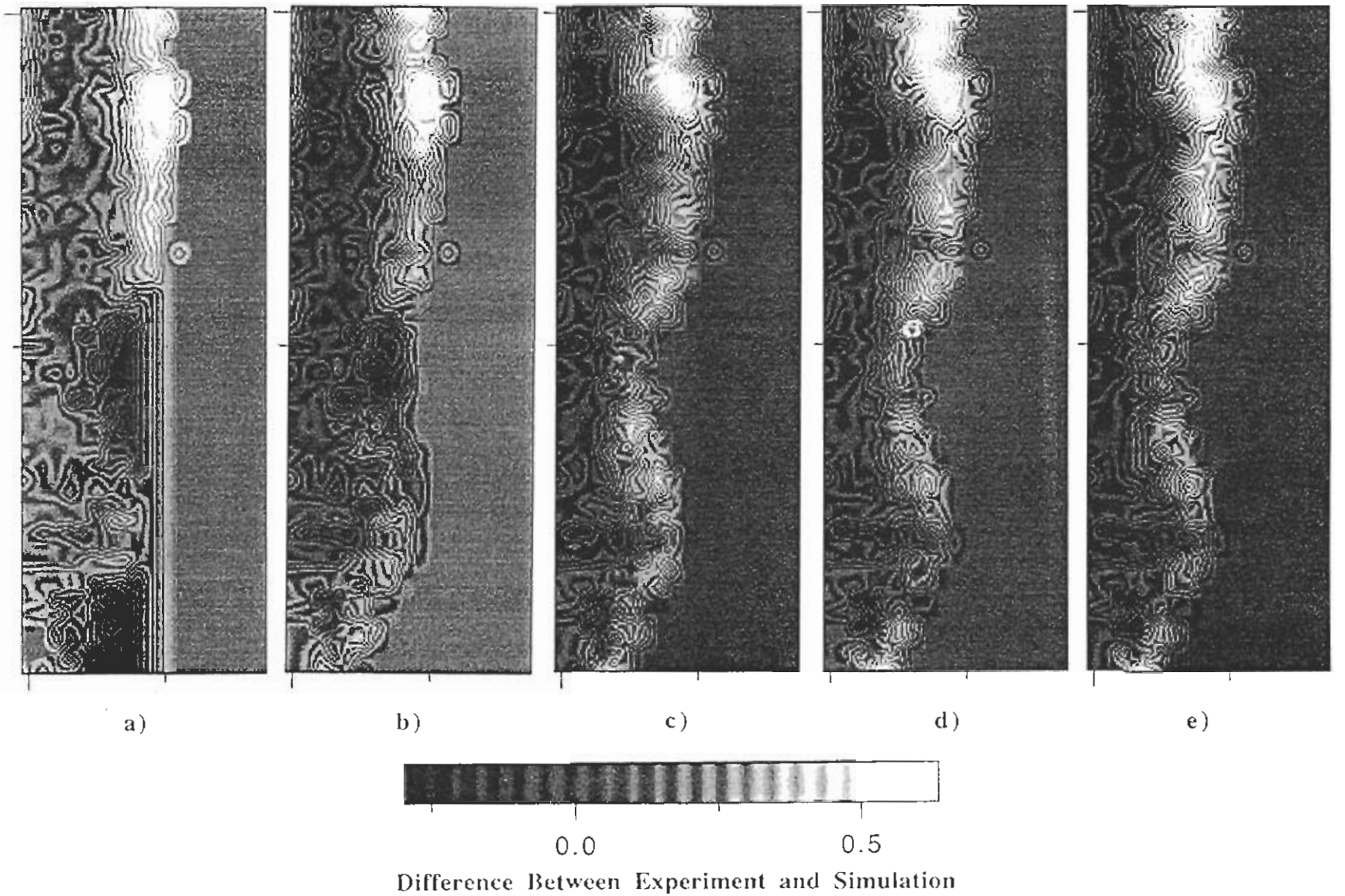

Figure 9: Difference fields between experimental saturations and simulated saturations for the a) 1, b) 3, c) 5, d) 11, and e) 21 hydraulic property classes. Bright areas indicate under prediction of saturation and dark areas indicate over prediction.

include a limit for liquid saturation due to air entrapment. Air entrapment occurred in our experiment as it does in all experiments where non-deaired water is used. As is shown by the band structure (depicting contours), heterogeneity in the saturation field behind the wetting front is much greater in the experiment than in the simulations.

The simulation based on the single hydraulic property class (Figure 9a) yields a one dimensional profile which, when compared with the data, does a remarkably good job at predicting the average location of the wetting front. Increasing detail in the property field up to 5 classes allows us to better simulate the wetting front shape. However, increased detail in the property field past 5 classes did not increase our ability to match the wetting front shape or location. In general, simulations predict smoother saturation profiles near the wetting front while the experiment exhibits sharper fronts.

DISCUSSION

In this study, laboratory measurements of hydraulic properties were limited in number (10) but covered a wide range of porosity and saturated conductivity. The correlation between porosity and van Genuchten fitting parameters, alpha and n, was not as strong as between porosity and the hydraulic conductivity (Figure 5); none-the-less, the correlations provided a good estimate of the pressure/saturation function (the least square fit to the data and the predicted function were nearly identical as shown in Figure 6). In sensitivity studies using TOUGH2, simulated saturation fields were found to be much more sensitive to the saturated conductivity than either alpha, or n. Shifting the mean porosity from 0.20 to 0.19 yielded a factor of 0.5 decrease in conductivity and a consequential reduction of 0.5 in the velocity of the wetting front. This suggests that we may not need to know alpha and n very well compared to the saturated conductivity or porosity for modeling unsaturated flow in this tuff.

Detail in the heterogeneity field as varied by the number of classes spanning the porosity histogram was seen to be influential only up to 5 hydraulic property classes with increasing detail yielding only marginal differences. While the simulations are remarkably close to the physical experiment, parameters could be adjusted by hand to achieve a better fit. For example, by including a liquid saturation limit, S_l ("satiated" value) that is dependent on the porosity with the value decreasing from 1.0 at the lowest porosity class to .85 above the average porosity class, the saturation field can be matched much better. However, including S_l without modifying the saturated K values measured under truly saturated conditions is not physically reasonable. Using the relative permeability relations estimated by the method of Mualem[12], the satiated K should be from 30 to 40% less than the value used to generate Figure 7a. Simulations with comparable reductions in conductivity show a decrease in saturation field development of 30 to 40%.

Our ability to modify model parameters to fit the data emphasizes the large number of parameters and assumptions that have gone into this comparison of physical experiment and numerical simulation. There are both assumptions in our experimental measurements and in our models. Focusing on modeling assumptions we have: 1) fitted discrete points for pressure saturation curve data with a functional form given by the van Genuchten[11] model; 2) used the drainage pressure/saturation curve for modeling imbibition where we should use the wetting curve; 3) used Mualem's[12] method to predict relative permeability; 4) used saturated values for K instead of satiated values; 5) used correlations between porosity and hydraulic properties to distribute properties within the blocks; 6) treated the rock slabs as heterogeneous but isotropic; 7) considered the fracture to be fully saturated; and 8) assumed that the KI solution does not affect the hydraulic properties of the tuff.

With such a broad list of assumptions we must be very careful in interpreting our "good match" between numerical simulation and the physical experiment for model validation. Many of these assumptions have yet to be tested independently and a lucky combination of errors could easily lead to misinterpretation. Beyond this, comparison of experimental results with numerical simulation for this problem does not constitute full model validation within the context of the Yucca Mountain Project as it does not test the model within the full range of boundary conditions or system parameters expected at Yucca Mountain. For example, the influence of fracture coatings and fracture and fracture network properties on fracture-matrix interaction have yet to be incorporated into experimentation.

CONCLUSION AND FUTURE WORK

The current experiment which combines state of the art hydraulic property measurement techniques, two-dimensional high resolution transient saturation field imaging techniques and numerical modeling, has produced new insight in understanding, characterizing, and modeling unsaturated flow in volcanic tuff. For example, if porosity is indeed well correlated to the saturated conductivity and we can show through transient tests such as our fracture/matrix experiment that it is the most sensitive parameter, then incorporating the deterministic trends in porosity found at Yucca Mountain[13] may facilitate estimating hydrologic properties across the site. In addition, porosity and saturated hydraulic conductivity are much more easily and inexpensively measured than pressure/saturation curves.

Issues of property scaling, however, must also be addressed. Our experiment is a scale up from small core scale to bench scale (1:70 scale up), and has been conducted under well controlled conditions. Under these conditions, extraneous effects common in field experiments due to lack of boundary/initial condition control and decreased resolution of data measurement will not lead to erroneous interpretations. Because of the low conductivity of the tuffs under

investigation and the tendency of fractures to create capillary barriers and inhibit flow under many unsaturated conditions, it is unlikely that we will be able to conduct unsaturated flow tests at scales much greater than a meter. This creates difficulties for the development and validation of experimentally based property scaling laws for use in large scale performance assessment calculations. In our opinion, the only viable option is to develop scaling laws through numerical exercises on problems up to tens of meters. Such an approach requires that we first adequately test our conceptual models with representative physical models at scales up to a meter, where experimentation is possible. Secondly, we must test our upscaled models on field scale natural analogues that are the result of thousands of years of naturally occurring "field tests".

To begin this task, we plan to conduct a series of studies where a number of fracture-matrix system parameters will be varied within the context of the proposed repository horizon rock, Topopah Spring Tuff. Experiments will be conducted at the current scale (approximately 0.25 m) and at the meter scale; at both scales a series of systems with increasing complication will be considered. First, orientation of single fractures with respect to matrix anisotropy will be examined in both unsaturated and saturated (solute transport/matrix diffusion) conditions. These experiments will progress from saw cut fractures to break fractures to natural fractures, with and without mineralogical coatings. Following these experiments on single fractures, a series of fracture networks within the matrix will be explored. In addition, nonisothermal conditions will be considered through collaboration with other Yucca Mountain participants.

REFERENCES

1. K. Pruess, TOUGH2 -- A General-Purpose Numerical Simulator for Multiphase Fluid and Heat Flow, LBL-294000, Lawrence Berkeley Laboratory, Berkeley, CA, 1991.

2. R.W. Barnard, M.L. Wilson, H.A. Dockery, J.H. Gauthier, P.G. Kaplan, R.R. Eaton, F.W. Bingham, and T.H. Robey , "TSPA 1991: An Initial Total-System Performance Assessment for Yucca Mountain", SAND91-2795, Sandia National Laboratories, Albuquerque, NM, (1992).

3. R.R. Peters, and E.A. Klavetter, "A Continuum Model for Water Movement in an Unsaturated Fractured Rock Mass", Water Resources Res., vol. 24, no. 3, 416-430, March (1988).

4. R.J. Glass, and V.C. Tidwell, "Research Program to Develop and Validate Conceptual Models for Flow and Transport Through Unsaturated, Fractured Rock", Proceedings of the Second Annual International Conference on High Level Radioactive Waste Management, Las Vegas, Nevada, April 28-May 3, (1991).

5. M.J.Nicholl, R.J. Glass, and H.A. Nguyen, "Gravity-Driven Fingering in Unsaturated Fractures", Proceedings of the Third Annual International Conference on High Level Radioactive Waste Management, Las Vegas, Nevada, April 12-16, (1992).

6. M.J. Nicholl, R.J. Glass, and H.A. Nguyen, "Small-Scale Behavior of Single Gravity-Driven Fingers in an Initially Dry Fracture", Proceedings of the Fourth Annual International Conference on High Level Radioactive Waste Management, Las Vegas, Nevada, April 26-30, (1993a).

7. M.J. Nicholl, R.J. Glass, and H.A. Nguyen, "Wetting Front Instability in an Initially Wet Unsaturated Fracture", Proceedings of the Fourth Annual International Conference on High Level Radioactive Waste Management, Las Vegas, Nevada, April 26-30, (1993b).

8. R.J. Glass and D.L. Norton, "Wetted Region Structure in Horizontal Unsaturated Fractures: Water Entry Through the Surrounding Porous Matrix", Proceedings of the Third Annual International Conference on High Level Radioactive Waste Management, Las Vegas, Nevada, April 12-16, (1992).

9. S.D. Foltz, V.C. Tidwell, and R.J Glass, "Investigation of Fracture-Matrix Interaction: Preliminary Experiments in a Simple System", Proceedings of the Fourth Annual International Conference on High Level Radioactive Waste Management, Las Vegas, Nevada, April 26-30, (1993).

10. V.C. Tidwell, and R.J Glass, "X-Ray and Visible Light Transmission as Two-Dimensional, Full-Field Moisture Sensing Techniques: A Preliminary Comparison", Proceedings of the Third Annual International Conference on High Level Radioactive Waste Management, Las Vegas, Nevada, April 12-16, (1992).

11. M. Th. Van Genuchten, "A Closed-Form Equation For Predicting the Hydraulic Conductivity of Unsaturated Soils", Soil Science Soc Am. J., vol. 44, 892-898, (1980).

12. Y. Mualem, "A new model for predicting the hydraulic conductivity of unsaturated porous media", Water Resources Res., vol. 12, 513-522, (1976).

13. C.A. Rautman, J.D. Istok, A.L. Flint, L.E. Flint, M.P. Chornack, "Influence of Deterministic Geologic trends on Spatial Variability of Hydrologic Properties in Volcanic Tuff", Proceedings of the Fourth Annual International Conference on High Level Radioactive Waste Management, Las Vegas, Nevada, April 26-30, (1993).